Monitoring land cover dynamics utilizing a change vector analysis approach: a case study of al Najaf Province, Iraq

Ebtihal T AL-Khakani[1, *]; Huda M. Hamid[2]

[1]*Dept. of Physics, College of Education for Girls, University of Kufa al Najaf, Iraq*
[2] *Dept. of Soil and Water Resources, College of Agriculture, Al-Qasim Green University, Babylon, Iraq*

**Corresponding author: csiw512@gmail.com*

Abstract

Analysing information relevant to land cover changes is a fundamental issue in studies linked to environmental diversity. The use of multi-time satellite images at different scales allowed continuous observation of land cover changes. Due to significant changes in land cover, specifically in the decades 2000–2010 and 2010–2020, al Najaf Province was selected as the study area. This work aimed to study changes in land cover in Al Najaf Province from satellite imagery, using change vector analysis (CVA), through the last two decades (2000–2010 and 2010–2020). The enhanced vegetation index 2 (EVI2) and the dry bare soil index (DBSI) represented the vegetation and soil condition in the study region. They were estimated via images from the satellite Landsat-5 TM for March for the two years 2000 and 2010, and Landsat 8 OLI 2020 for the same month, then were considered the parameters for a land cover change analysis using the CVA. The outputs of the CVA were assessed on maps of land cover obtained through the supervised classification for the above-mentioned images. The results of the change vector magnitude found that the ratio of the changed area reached 46.58% and 56.35%, and the unchanged area was 53.42% and 43.65% for the periods (2000–2010) and (2010–2020), respectively. The results of the change direction revealed that the moisture reduction ratio was 26.93% and 4.85%, while the vegetation regrowth ratio was 15.81% and 38.79% for the same two periods, respectively. The results of the two periods considered exhibited that the EVI2-DBSI combination presented promising performance results with the overall accuracy of 0.90 and 0.92 and a kappa index of 0.867 and 0.852, respectively. As a result, the CVA technique offers a promising way to track environmental changes that are connected to the dynamics of land use/land cover in this region.

Keywords: Change vector analysis; dry bare soil index; enhanced vegetation index 2; land cover change; Landsat.

1. Introduction

The phrase land cover is often used to describe the general biophysical state of the land surface as well as giving information on the distribution of vegetation, water, soil, etc. The changes in

land cover resulting from several human and natural factors, represented by the changes of relative biophysical characteristics of the Earth's surface, have significant effects on the quality of environmental systems. So, the changes in the cover of land can represent the principal indices of environmental changes at various temporal and spatial scales (Polykretis *et al*., 2020).

The survey of land cover/use change is significant for the management of natural resources in the regional and local areas of the country (Sangpradid, 2018). Change detection may be defined as a methodology for distinguishing variations in the status of a target or phenomenon by monitoring them at various times (Tong *et al*., 2020). For studying the land cover changes of a particular area, it is essential to obtain the information that reveals its condition at different time intervals (Polykretis *et al*., 2020). Change detection utilising satellite imagery and a GIS platform is an effective method (Mohammed, 2021), where it is characterised by quickly collecting multi-spatial data and a multi-temporal resolution that allows the mapping of changes of land cover at various levels (Tong *et al*., 2020).

Depending on the methods of processing data for change detection, the techniques used were divided, according to Johnson & Kasischke (1998), into two major groups: (a) depending on the input data's spectral categorisation (classification) and (b) techniques that build on the radiometric changes for data with different dates, like band ratio, band difference, image difference obtained from band conversion (e.g., vegetation and soil indicators) and change vector analysis (CVA).

Vegetation cover or bare soil are often indicated as biophysical characteristics of the land surface. These characteristics can be measured using several spectral indices for vegetation and soil (Islam *et al*., 2016). The spectral indicators describe the conditions of vegetation and soil cover, respectively, for a particular area, employing a specific value range depending on the level of absorption/reflection from the surface of the Earth in the various parts of the electromagnetic spectrum or satellite bands (Münch *et al*., 2019). The relation between the spectral indicators and change detection of land cover is well established as a result of their commonly used application in this type of analysis.

The CVA technique has been employed by many researchers to study land cover changes, for example, detecting changes in the forests (Malila,1980), detecting the change of land cover in rural-urban regions (He *et al*., 2011), evaluating humid land dynamics (Landmann *et al*., 2013), detecting the changes in agricultural land use (Aravind, S., & Sivakumar, R.2016), observation of the changes of fuzzy shorelines (Dewi *et al*., 2017), and monitoring forest resources (Xiao-hui *et al*., 2021). The CVA method allows the user to classify various kinds of change concerning land cover dynamics in a given region (Ebrahimian, R., & Alesheikh, A. 2019). It provides the possibility to determine the nature of the change, in addition to its magnitude, where it is a powerful tool for detecting radiometric changes (Fernandes *et al*., 2014).

This research aims to detect the changes in land cover of Al Najaf Province employing the CVA technique. The CVA technique was applied using EVI2 and DBSI indices from Landsat satellite data for the two periods 2000–2010 and 2010–2020.

2. Materials and Methods

2.1. Study Site

Al-Najaf Province is situated in the southwest part of Iraq, at 70 m above sea level. It is 160 km from the capital, Baghdad, with an area of about 28,824 km^2. The study zone represents the north-eastern portion of the province (figure 1), with an area estimated at 2,112 km^2, and lies between latitude 31º 37′–32º 21′ N and longitude 44º 7′– 44º 37′ E. The area selected for the study includes the land cover types that experienced significant changes in the period 2000–2020. The region witnessed the transformation of significant parts of bare lands and agricultural areas into urban areas, in addition to considerable changes in water areas as a result of the large variation in total annual rainfall from 2000 to 2020 (General Authority for Meteorology) ,as indicated in figure 2, which influenced the large variations in vegetation cover.

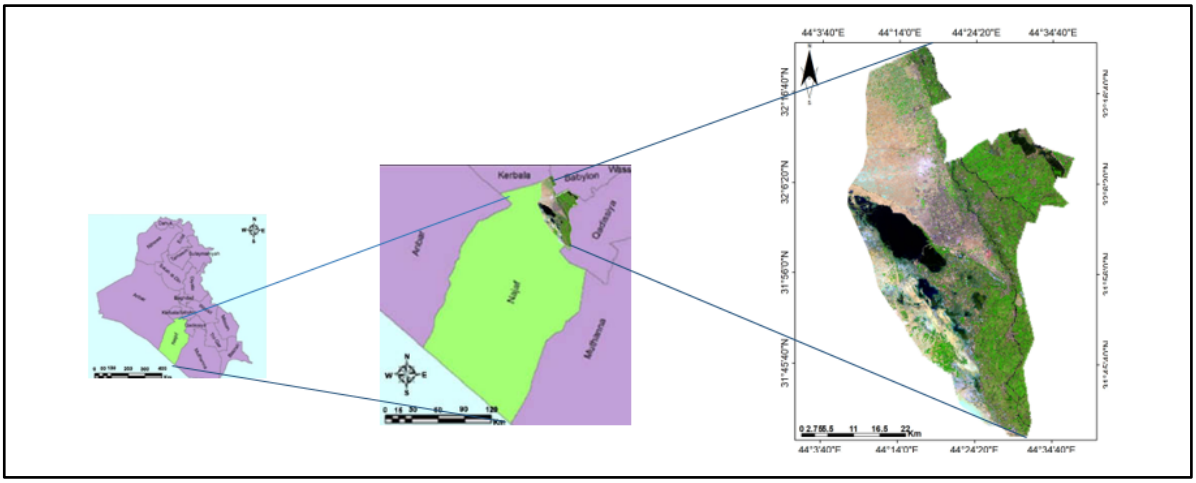

Fig. 1. Study area site. From left to right: location of al Najaf Province in Iraq, study site in al Najaf province and Landsat image (2020) for the study area (band combination RGB 3, 5, 7).

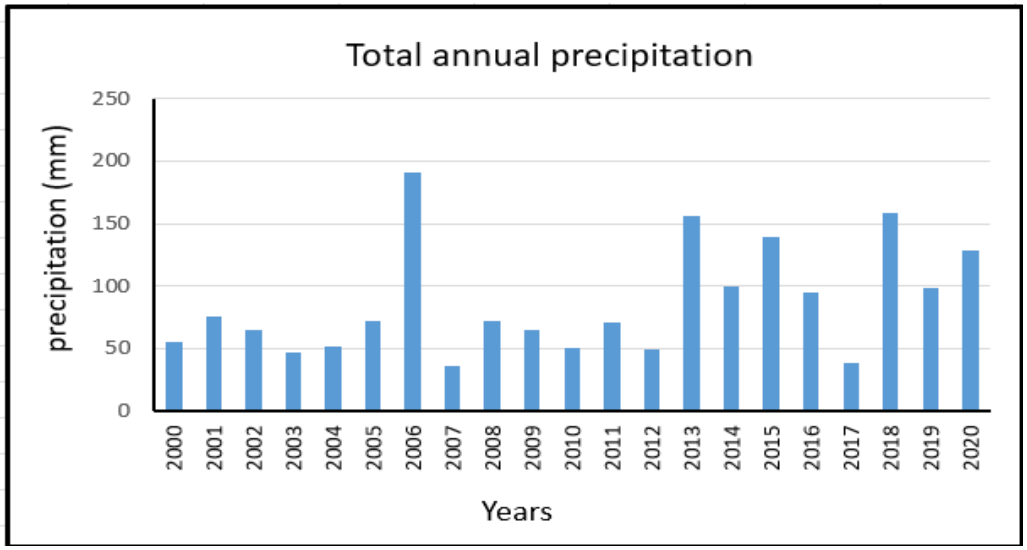

Fig. 2. Total annual precipitation for the period from 2000 to 2020.

2.2. Data utilised

In this research, Landsat satellite images for the period 2000–2020 were selected to assess the changes in the land cover of the study region. The time period was chosen based on the significant changes that occurred in the land cover and the availability of appropriate data for that period. All images, downloaded from http://landsat.usgs.gov, were cloud-free and were systematically rectified at downloaded. The multi-spectral imagery data with a resolution of 30 m were obtained for the Landsat-5 TM in March 2000 and 2010, and Landsat 8 OLI in March 2020, path/row 168/38. The data have been corrected to a Universal Transverse Mercator (UTM) projection via the WGS84 datum and zone 38. The dates of the images were chosen as they represent the peak of the vegetation growing season in the region (from March to May). The images for the three years were from the same month to reduce seasonal variation. Arc GIS 10.6 software was employed for pre-processing data, and Excel 2019 was utilised for the other analyses.

2.3. Spectral indices used

To evaluate the biophysical characterisation of the study region, two spectral indices have been employed after processing Landsat imagery data.

For measuring the changes of land cover for the studied region, the enhanced vegetation index 2 (EVI2) to describe vegetation conditions, and the dry bare soil index (DBSI) to describe the soil conditions of the zone, were computed from Landsat images. EVI2 is an improved version of NDVI. It reduces atmospheric effects, and it can be formulated according to the equation as follows (Jiang *et al*., 2008):

$$EVI2 = 2.5 \frac{\rho_{NIR} - \rho_{RED}}{\rho_{NIR} + 2.4 * \rho_{RED} + 1} \quad (1)$$

Where ρ_{NIR} and ρ_{RED} are the values of surface reflectance for near-infrared and visible red bands (Landsat-5 TM bands 4 and 3, and Landsat 8-OLI bands 4 and 5, respectively).

The EVI2, similar to NDVI, is a unit less variable, whose values range from -1 to 1. The value of 2.5 is the gain factor, the coefficient 2.4 is employed to reduce aerosol impacts and the value of 1 represents the soil adjustment factor utilised to reduce soil background influences.

The DBSI, created by Rasul *et al*. in 2018, improves differentiation between dispersed vegetation and bare soil to identify bare zones in dry climates. The values of the DBSI range from -2.0 to +2.0. The higher value is conformed to the bare soil area. The proposed formula for the DBSI is (Rasul *et al*., 2018):

$$DBSI = \frac{\rho_{SWIR1} - \rho_{Green}}{\rho_{SWIR1} - \rho_{Green}} - NDVI \quad (2)$$

2.4. Change vector analysis

CVA is a change detection method that exhibits the change as a vector, either in two- or multi-dimensional space. The idea of CVA includes the computation of spectral changes according to multi-temporal pairs of spectral indicators (Fernandes & Almeida, 2014). The computed change

vector involves basic information about the magnitude and direction of change, where it allows for mapping them between the dates specified, pixel by pixel (Polykretis *et al*., 2020).

If two components are used, the two-dimensional space is represented with two axes via a Cartesian coordinate system. The change vector consists of two points corresponding with the same pixel at two different times, where the beginning and ending points represent the pixel positions in EVI2-DBSI space on these two dates (Sangpradid, 2018). The change magnitude (M) is measured between the first (t1) and second (t2) dates, across the length of the change vector as in figure 3A where it is calculated utilising the Euclidean distance according to the formula:

$$M = \sqrt{(EVI2_{t2} - EVI2_{t1})^2 + (DBSI_{t2} - DBSI_{t1})^2} \quad (3)$$

Where $EVI2_{t1}$ and $EVI2_{t2}$ are the pixel values of the EVI2 index at the two dates of t1 and t2, respectively. As well, $DBSI_{t1}$ and $DBSI_{t2}$ are the values of pixels for the DBSI index for the same two dates.

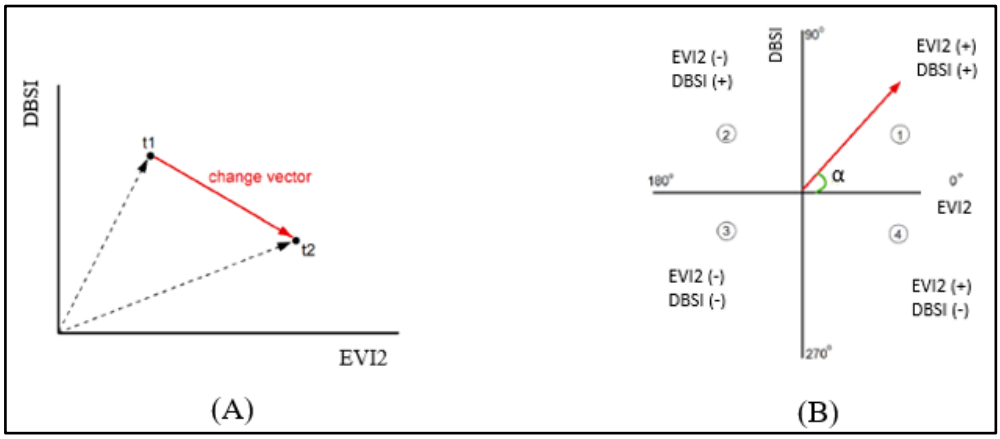

Fig. 3. The change vector analysis for space of EVI2-DBSI,
(A) the magnitude of change and (B) the direction of change.

A threshold is set according to standard deviations for the values of magnitude to differentiate between changed and unchanged portions from the study region. The direction of change is determined by computing the change vector angle, which varies with the number of components utilised. This angle refers to the kinds of changes that have occurred during two particular dates (Fernandes & Almeida, 2014), which describes the type of change concerning the directions of mutual change within the pixel units of the two components. In general, the number of direction classes is equivalent to 2n, where n represents the number of components or spectral bands (Karnieli *et al*., 2014). In this paper, two components (DBSI and EVI2) were employed as input, so the direction of change is classified into four categories of angles, or four quadrants, as shown in figure 3B. The change vector direction was calculated in a two-dimensional space, using the following equation:

$$\tan \alpha = \frac{DBSI_{t2} - DBSI_{t1}}{EVI2_{t2} - EVI2_{t1}} \quad (4)$$

Where, tan(α) represents the tangent of angle α.

Based on the directions of change within pixels in the DBSI and EVI2 components: Angle measurements between 0º–90º indicate an increase in both bands. The angles between 90º–180º represent an increase in the EVI2 and a decreased DBSI. Angle measurements between 180º–270º indicate a decrease in both components. Finally, the angles between 270º–360º refer to a decrement in EVI2 and an increase in DBSI (Fernandes & Almeida, 2014).

2.5. Methodology

In this research, the CVA technique has been applied to reveal the changes in land cover using two spectral indices, EVI2 and DBSI. The changes in magnitude in land cover for the studied area for the two periods 2000–2010 and 2010–2020 were estimated utilising equation (3) in ArcGIS software. Relying on prior expertise in change detection analysis, the standard deviation (ST) by the value of one from the average, has been specified as a threshold (Bayarjargal *et al*., 2006; Paz-Kagan *et al*., 2014; Volcani *et al*., 2005) for a distinction between changed and unchanged regions. In a similar way, the change level has been classified into low change and high change. The results of the change magnitude are displayed as maps graded into three classes: high change, low change and no change, for the two periods 2000–2010 and 2010–2020. The change direction has been determined based on the angles of the change vectors using equation (4).

Each of the four angle categories is associated with types of land cover changes for the study region. The angles 0º–90º represent the increment in both the EVI2 and DBSI indices. This category identifies areas of varying biomass or low humidity and is often associated with changes in agricultural zones. The angles 90º–180º, which correspond to a decrease of the EVI2 indicator and an increase of the DBSI indicator, represent the extension of bare soil or degraded areas. The angles 180º–270º, which conform to a decrease in both spectral indicators, represent water bodies or increased humidity. The range angles 270º–360º are connected with an increase and a decrease of the EVI2 and DBSI indicator values, respectively, which indicates the re-growth of vegetation cover, i.e., areas that experienced an improvement in land quality (Karnieli *et al*., 2014).

3. Results

3.1 The results of the EVI2 and the DBSI

The results of the EVI2 and the DBSI were assessed for the 2000, 2010, and 2020 Landsat imagery data. Figure 4 shows the results of the EVI2 for 2000, 2010, and 2020. The area of vegetation cover was lower in 2010 than it was in 2000, specifically in the south-eastern section of the region, while in 2020, vegetation increased in most eastern and south-eastern parts of the studied zone. Figure 5 displays the DBSI results for the period 2000–2020. The low values of the DBSI have accompanied the areas with a high vegetation density.

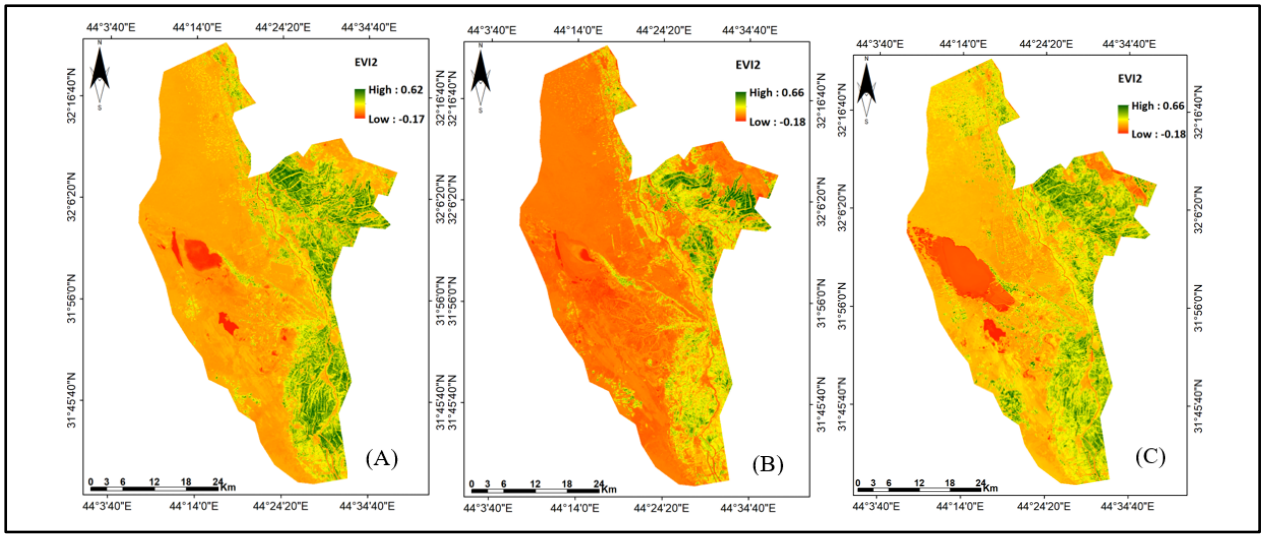

Fig. 4. Results of the enhanced vegetation index 2 for years (A) 2000, (B) 2010, and (C) 2020

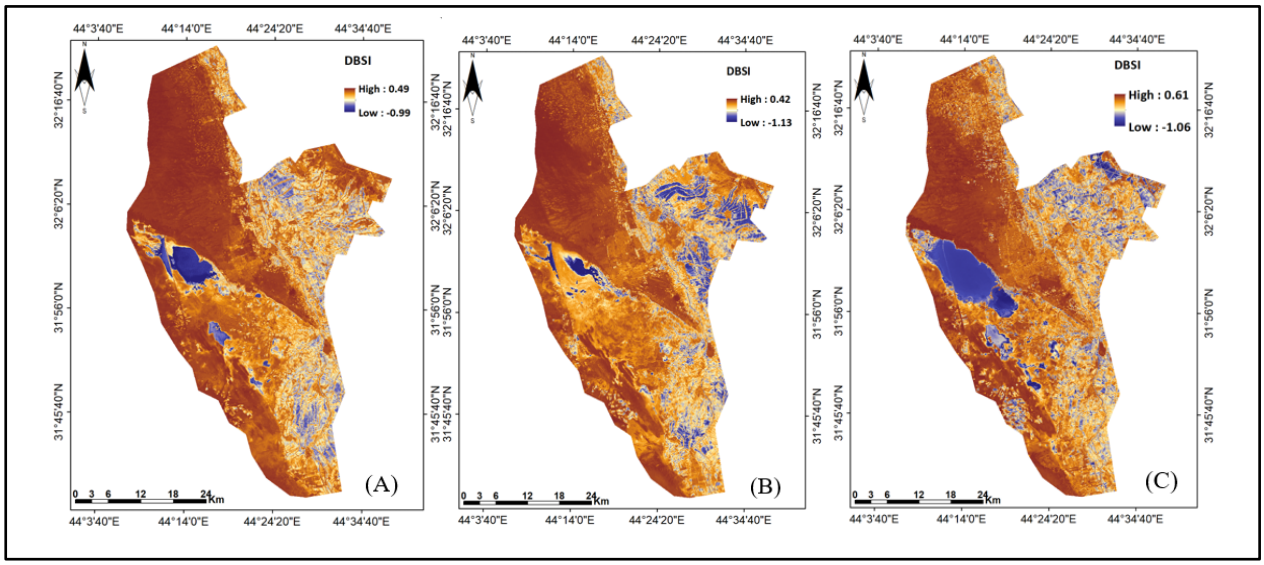

Fig. 5. Results of the dry bare Soil index for years (A) 2000, (B) 2010, and (C) 2020

3.2 Analysis of CVA

The outcomes of CVA have two parameters: the change magnitude and the change vector direction. Figure 6 A and B illustrate the maps of change magnitude generated by the EVI2-DBSI combination for the two periods 2000–2010 and 2010–2020.

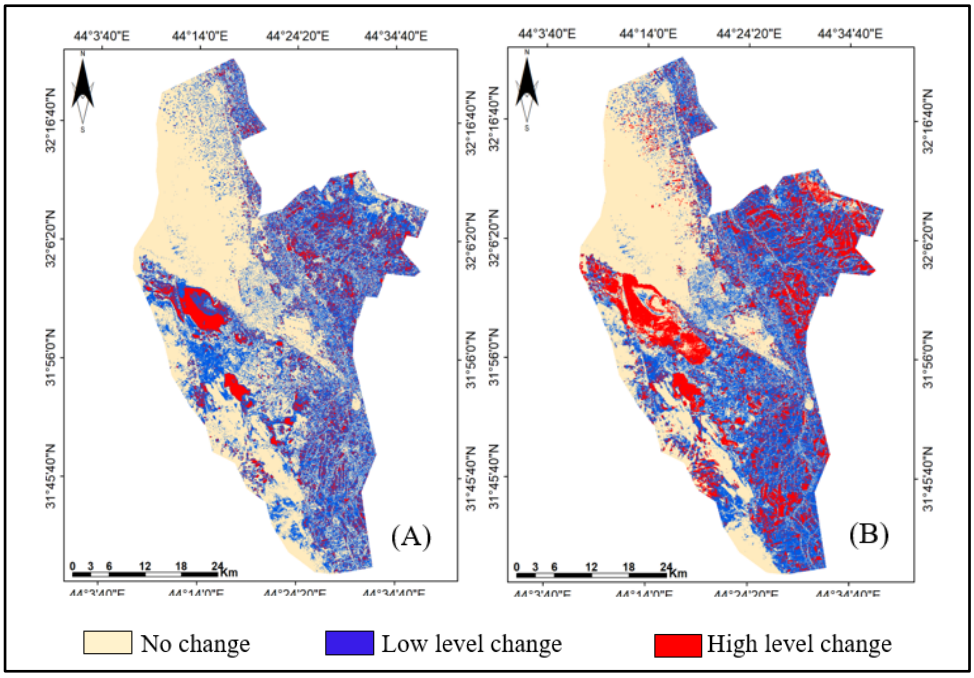

Fig. 6. Maps of change magnitude (A) for the period 2000–2010 and (B) for 2010–2020 from EVI2-DBSI combination.

Between 2000 and 2010, about 46.58% (983.9 km^2) of the study region suffered changes, as against 53.42% (approximately 1,128.54 km^2) unchanged, as in figure 6A. The area with low-level changes reached 754.76km^2, while high-level changes were 229.14 km^2, which were concentrated in the western section of the study site in the Bahr Al-Najaf depression and some of the zones of agricultural fields.

From 2010–2020, many changes occurred in large parts of the study site compared to the 2000–2010 period, as illustrated in figure 6B. Land totalling 56.35% (approximately 1,190.82 km^2) witnessed a change, while the rest, about 43.65% (921.82 km^2) showed no change. Of the total changing area, 36.4% (about 769.02 km^2) was associated with low-level changes, observed in most agricultural land, and 19.95% (about 431.54 km^2) had high-level changes, which were mainly concentrated in water zones as well as a few areas of bare soil.

Concerning the direction of change from 2000 to 2010, figure 7A, nearly 26.93% (approximately 577.33 km^2) of the study zone suffered biomass variation/moisture reduction, followed by about 15.81% (334.06 km^2) that experienced regrowth of vegetation cover, and 2.75% (approximately 31.60 km^2) witnessed a bare soil expansion. A small portion of the study zone equal to 1.09% (approximately 23.02 km^2) showed a water body/moisture increase.

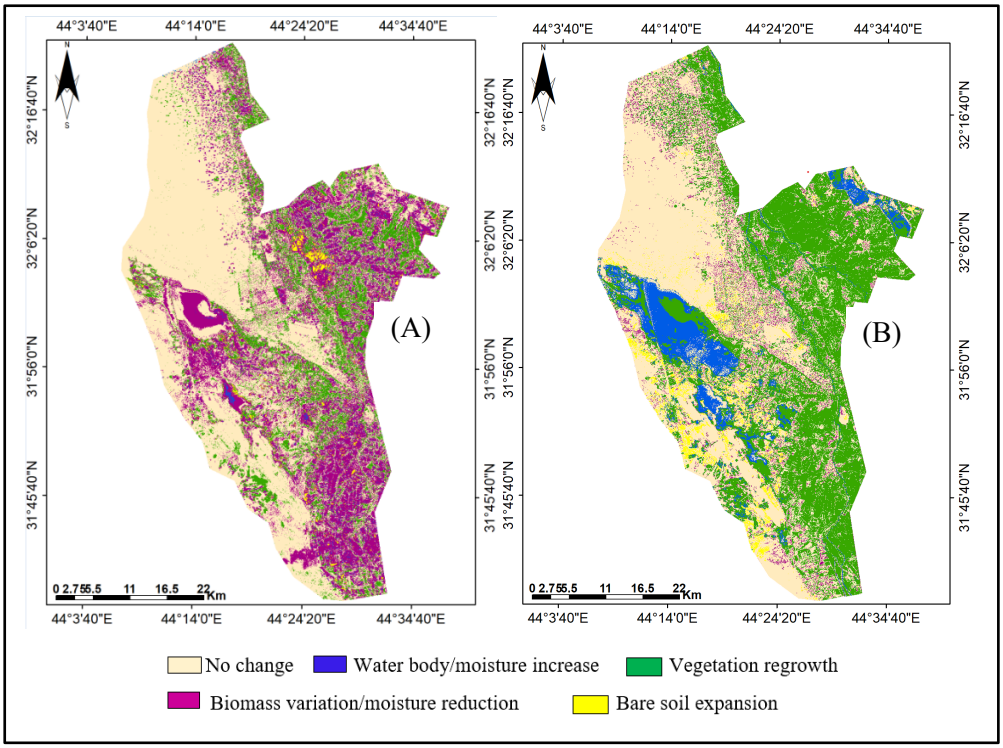

Fig. 7. Maps of change direction, left, for 2000–2010, and on the right, for 2010–2020, from EVI2-DBSI combination.

According to the change directions for the period 2010–2020 (figure 7B), a large part of the study area witnessed about 38.7% (5,096 km^2) of vegetation regrowth, according to the scattered spatial coverage of vegetation cover. There was an increase in water bodies/moisture of approximately 8.92% (183.08 km^2). A less extensive part, which is 4.85% (about 100.5 km^2), suffered a biomass variation/moisture reduction. Finally, the expansion of bare soil increased slightly, around 3.79% (approximately 67.03km^2). Figures 8 and 9 show the percentage of change magnitude calculated for the relative categories for each period.

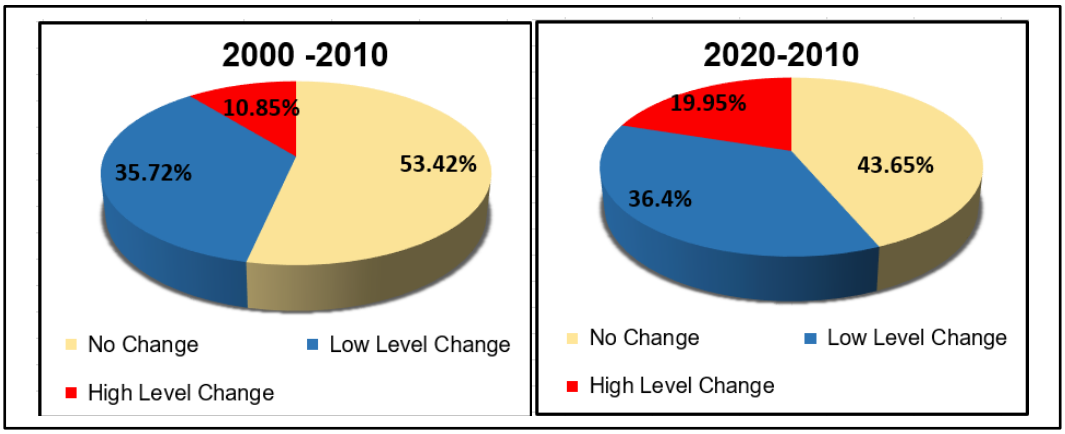

Fig. 8. Percentages of change magnitude classes for the two study periods.

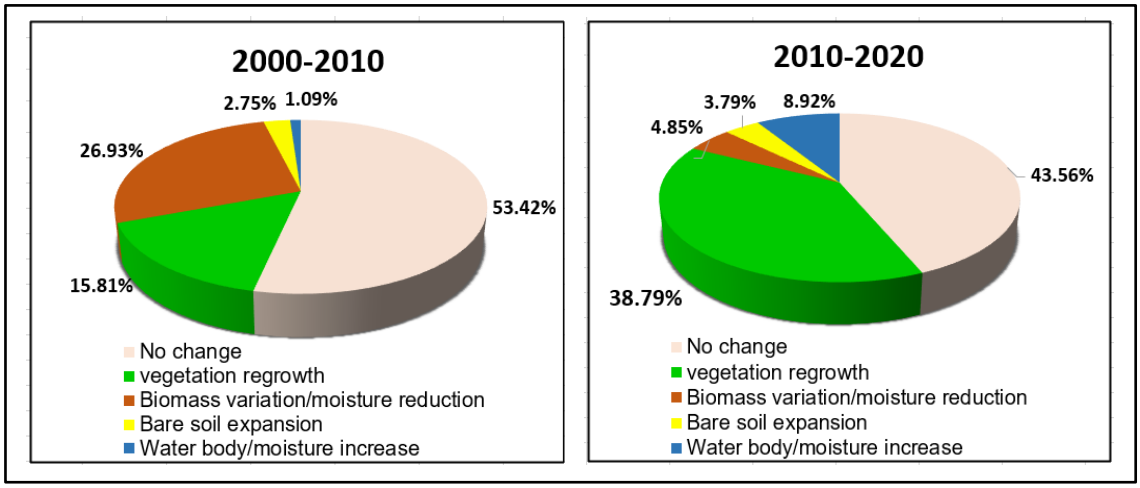

Fig. 9. Percentages of change direction classes for the two study periods.

3.3 Accuracy assessment

Accuracy evaluation of the CVA outputs was performed using the error (or confusion) matrix for defining the overall accuracy, and the kappa index (Equations 5 and 6) (Thakkar *et al*., 2017; Keshtkar & Alizadeh, 2017) was used to test the accuracy of results and compare them with actual reality. The confusion matrix is a two-dimensional table that enables the performance of an image classification method to be visualised. The truth data is represented by the table's columns (x-axis), while the classified image results are represented by the rows (y-axis) (or vice versa) (Congalton, 1991). The kappa coefficient ranges from 0 for very low accuracy to 1 for excellent accuracy. Because precise field-derived data was unavailable, new data produced through remote sensing was developed to establish reference data. It was generated utilising a supervised classification of Landsat satellite images to create detailed maps of land cover. On composite RGB colour images of 2000, 2010, and 2020, about 246 random sample zones were collected. Visual interpretation was used to designate these locations as a distinct land cover type, resulting in a total of five categories being represented. ArcGIS software was used to create a detailed map of land cover for each date, using the identified areas and a supervised classification method through a maximum likelihood classifier (MLC). The maximum-likelihood algorithm locates the likeness with an unknown data item and a defined dataset via a covariance matrix depending on the correlations within a dataset and the data distribution. To determine changing or non-changing regions through the periods 2010–2000 and 2020–2010, spatial analysis based on GIS was performed for pairs of these maps. The type of change was then assigned and named based on the change direction classes of CVA. Finally, for obtaining the statistics of overall accuracy and the kappa index, the specified information as reference data was compared with the outputs of CVA (the magnitude and direction of change) in confusion matrices.

$$Overall\ accuracy = \frac{Total\ number\ of\ correct\ samples}{Total\ number\ of\ samples.} \times 100 \quad (5)$$

$$K = \frac{(The\ diagonal\ elements\ sum \times sum\ of\ correct) - sum\ all\ of\ the\ (row\ total \times column\ total)}{Total\ of\ correct\ squared - sum\ of\ all\ the\ (row\ total \times column\ total)} \quad (6)$$

Table 1. The values of overall accuracy and kappa coefficient for the two time periods.

Period	Change/No Change (Magnitude)		Kind of Change (Direction)	
	Overall Accuracy	Kappa Index	Overall Accuracy	Kappa Index
2000-2010	0.901	0.849	0.885	0.867
2010-2020	0.921	0.879	0.829	0.852

4. Discussion

In this work, through the application of the CVA technique utilising two EVI2 and DBSI indexes, the land cover changes were located and evaluated for the time intervals 2000–2010, and 2010–2020. Vegetation and soil indicators were created based on images from the Landsat satellite obtained for March 2000, 2010, and 2020. CVA is a promising technique for observing the changes of land cover, with the ability to provide important qualitative and quantitative information regarding the dynamics of temporal and spatial land cover. The results of the CVA outputs (magnitude and direction of change) allow various magnitudes and types of change to be determined.

Compared to classification-based methods, the CVA technique can simultaneously analyse a combination of remotely sensed data to monitor the changes within categories of land cover. Such changes are obtained by observing the variation between consecutive satellite images without going into an uncertain classification (Karnieli *et al*., 2014).

The CVA results of the DBSI-EVI2 combination were mapped to define the spatial distribution for the change magnitudes and the types of land cover changes in the studied zone. The maps of magnitude in figures. 5A & B, showed that, for both periods evaluated, most of the study region was influenced via low-level changes. In addition, large areas remained unchanged. The high-level changes were significantly low in 2000–2010, but clearly increased in 2010–2020.

According to the change direction maps in figure 6A, the study area generally experienced a marked decrease in vegetation cover during the period 2000–2010. Indicating the decrease in regrowth areas at the expense of a raising in the degraded land area, that represent the biomass variations regions (or moisture reduction), where concentrated in the central, eastern, and south-eastern parts, with the expansion of bare soil areas. The spatial expansion of degraded or arid land can be attributed to reduced annual rainfall in this period (as illustrated in figure.2)

and droughts arising from poor land management. Also, the water bodies of the region, represented by the depression of Bahr Al-Najaf, witnessed a noticeable decrease in their levels during the same period due to the dwindling of the floodwaters that feed this depression.

Moreover, as seen in figure 6B, the period 2010–2020 witnessed an increase in regrowth zones, where cultivated areas expanded due to increased agricultural activity and rainfall levels rising from 50.3 mm in 2010 to 128.4 mm in 2020, as illustrated in figure 2. This was evident in the eastern and south-eastern portions of the studied region, where there was a significant decrease in areas of biomass variation/humidity reduction. Water bodies have expanded significantly compared to the previous period because of the increased flow of torrent water, which is the major source of water.

Confusion matrices have been utilised for evaluation of the accuracy of CVA outputs, based on change/non-change (magnitude) in addition to the type of change (direction), for the 2000–2010 and 2010–2020 periods. Table 1 offers the values of overall accuracy and the kappa coefficient calculated using these matrices, in accordance with (Landis, & Koch, 1977). These results are considered very acceptable.

5. Conclusion

Currently, remote sensing imagery and different analysis techniques provide further information to monitor and detect changes in land cover. CVA is a powerful and effective method to detect radiometric changes in the multi-spectral remote sensing data. The results of the CVA technique implementation using two components, EVI2 and DBSI, showed the ability to detect and classify different categories of changes concerning biomass gain and loss. The results demonstrated that the number of regions that did not change was higher than those with high-level and low-level changes through the two periods studied.

Between 2000 and 2010, there has been a decline in areas of regrowth and water bodies. From 2010 to 2020, regrowth zones and water bodies have increased as large areas of bare soil have shifted to agricultural use due to increased rainfall.

The CVA technique offered satisfactory results for the two study periods, as the overall accuracy of the final maps was 0.885 and 0.829, with a kappa index of 0.867 and 0.852 respectively, indicating that accurate change detection can be obtainable. The maps of change magnitude and direction could establish a fundamental rule for planners in determining changes of land cover and planning suitable land administration strategies.

ACKNOWLEDGEMENTS

The authors extend their thanks and great gratitude to Assistant Professor Dr. Khaleda Al-Mayali, Head of the Physics Department at the College of Education for Girls, University of Kufa, for her support and valuable comments.

References

Aravind, S., & Sivakumar, R. (2016). Agricultural land use change detection using change vector analysis in lower Velar Watershed. International Journal of Engineering Research & Technology, **4**(20), 1-6.

Bayarjargal, Y.; Karnieli, A.; Bayasgalan, M.; Khudulmur, S.; Gandush, C.; Tucker, C.J. (2006). A comparative study of NOAA-AVHRR derived drought indices using change vector analysis. Remote Sensing Environment, **105**(1), pp. 9–22.

Congalton, R. G. (1991). A review of assessing the accuracy of classifications of remotely sensed data. Remote Sensing of Environment, **37**(1), pp. 35–46.

Dewi R., Bijker W. and Stein A. (2017). Change Vector Analysis to Monitor the Changes in Fuzzy Shorelines. Remote Sensing, **9**(2), pp.1–28.

Ebrahimian, R., & Alesheikh, A. (2019). a Change Vector Analysis Method to Monitor Drought Using Landsat Data. The International Archives of Photogrammetry, Remote Sensing and Spatial Information Sciences, 42, 321-325.

Fernandes, P. J. F., & de Almeida Furtado, L. F. (2014). Change vector analysis to detect deforestation and land use/land cover change in Brazilian Amazon. Brazilian Geographical Journal: Geosciences and Humanities Research Medium, **5**(2), pp. 371–387.

General Authority for Meteorology and Seismic Monitoring / Climate Management / Republic of Iraq. Unpublished data.

He C., Wei A., Shi P., Zhang Q. and Zhao Y. (2011). Detecting land-use/land-cover change in rural-urban fringe areas using extended change-vector analysis. International Journal of Applied Earth Observation and Geoformation, **13**(4), pp. 572–585.

Islam, K., Jasimuddin, M., Nath, B., & Nath, T. K. (2016). Quantitative Assessment of land cover change using landsat time series data: case of Chunati Wildlife Sanctuary (CWS), Bangladesh. International Journal of Environment and Geoinformatics, **3**(2), pp. 45–55.

Jiang, Z., Huete, A. R., Didan, K., & Miura, T. (2008). Development of a two-band enhanced vegetation index without a blue band. Remote Sensing of Environment, **112**(10), pp. 3833–3845.

Johnson, R. D., & Kasischke, E. S. (1998). Change vector analysis: A technique for the multispectral monitoring of land cover and condition. International Journal of Remote Sensing, **19**(3), pp. 411–426.

Karnieli, A., Qin, Z., Wu, B., Panov, N., & Yan, F. (2014). Spatio-temporal dynamics of land-use and land-cover in the Mu Us sandy land, China, using the change vector analysis technique. Remote Sensing, **6**(10), pp. 9316–9339.

Keshtkar, H., Voigt, W., & Alizadeh, E. (2017). Land-cover classification and analysis of change using machine-learning classifiers and multi-temporal remote sensing imagery. Arabian Journal of Geosciences, **10**(6), pp. 1–15.

Landis, J. R., & Koch, G. G. (1977). The measurement of observer agreement for categorical data. *biometrics*, pp. 159–174.

Landmann T., Schramm M., Huettich C., and Dech S. (2013). MODIS-based change vector analysis for assessing wetland dynamics in Southern Africa. Remote Sensing Letters, **4**(2), pp. 104–113.

Malila, W. A. (1980). Change vector analysis: an approach for detecting forest changes with Landsat. In LARS symposia, pp. 326–335.

Mohammed, D. A. (2021). Integrated remote sensing and GIS techniques to delineate groundwater potential area of Chamchamal basin, Sulaymaniyah, NE Iraq. Kuwait Journal of Science, **48**(3), pp.1–16.

Münch, Z., Gibson, L., & Palmer, A. (2019). Monitoring effects of land cover change on biophysical drivers in rangelands using albedo. Land, **8**(2), pp. 1–28.

Paz-Kagan, T.; Panov, N.; Shachak, M.; Zaady, E.; Karnieli, A. (2014). Structural changes of decertified and managed shrub land landscapes in response to drought: Spectral, spatial and temporal analyses. Remote Sens. **6**(9), pp. 8134–8164.

Polykretis, C., Grillakis, M. G., & Alexakis, D. D. (2020). Exploring the impact of various spectral indices on land cover change detection using change vector analysis: A case study of Crete Island, Greece. Remote Sensing, **12**(2), pp,1–25.

Rasul, A., Balzter, H., Ibrahim, G. R. F., Hameed, H. M., Wheeler, J., Adamu, B., & Najmaddin, P. M. (2018). Applying built-up and bare-soil indices from Landsat 8 to cities in dry climates. Land, **7**(3), pp. 1–13.

Sangpradid, S. (2018). Change Vector Analysis using Integrated Vegetation Indices for Land Cover Change Detection. International Journal of Geoinformatics, **14**(4), pp.71–77.

Thakkar, K., Desai, V., Patel, A., & Potdar, M. (2017). Impact assessment of watershed management programs on land use/ land cover dynamics using remote sensing and GIS. Remote Sensing Applications: Society and Environment, Elsevier, 5, pp. 1–15.

Tong, S. S., Pham, T. L., Nguyen, Q. L., Le, T. T. H., Cao, X. C., Ahmad, A., & Tong, T. H. A. (2020). The Study of Land Cover Change Using Change Vector Approach Integrated with

Unsupervised Classification Method: A Case In Duy Tien (Vietnam). Geography, Environment, Sustainability, **13**(2), pp.175–184.

Volcani, A.; Karnieli, A.; Svoray, T. (2005). The use of remote sensing and GIS for spatio-temporal analysis of the physiological state of a semi-arid forest with respect to drought years. Forest Ecology and Management, 215, pp. 239–250.

Xiao-hui, W. A. N. G., Bing-xiang, T. A. N., Shi-ming, L. I., & Lin-yan, F. E. N. G. (2021). Object-oriented Forest Change Detection Based on Multi-feature Change Vector Analysis. Journal of Forest Research, **34**(1), 98-105

Submitted: 18/04/2021
Revised: 26/08/2021
Accepted: 02/11/2021
DOI: 10.48129/kjs.16391